THE ASTROPHYSICAL JOURNAL, 438:776–783, 1995 January 10

THE NGC 7538 IRS 1 REGION OF STAR FORMATION: OBSERVATIONS OF THE H66α RECOMBINATION LINE WITH A SPATIAL RESOLUTION OF 300 AU

R. A. GAUME[1,2] W. M. GOSS,[3] H. R. DICKEL,[4] T. L. WILSON,[5] AND K. J. JOHNSTON[1]
Received 1994 April 7; accepted 1994 July 15

ABSTRACT

The 1.3 cm continuum and the H66α recombination line emission toward NGC 7538 IRS 1 have been imaged with a spatial resolution of 180 and 300 AU, respectively. There are several remarkable aspects to the data. The core of the H II region is composed of numerous emission clumps with peak brightness temperatures of ≈15,000 K. Extremely wide line profiles, 250 km s^{-1} FWZP, are observed from the core, indicating substantial mass motions of the ionized gas. The H66α spectral profiles exhibit multiple emission peaks. The peaks and shapes of the H66α recombination line profiles vary significantly as a function of position within the core region. The H66α line-to-continuum ratios also vary considerably within the core region. A thin strip midway between the northern and southern core continuum components is the region of largest electron density. The center of this dense, disk-like structure most likely delineates the position of the exciting star.

We present a model for NGC 7358 IRS 1 that involves a stellar wind outflow and photoevaporation of nearby clumpy neutral material. This results in a clumpy continuum appearance and a complicated set of broad- and multiple-peaked spectral profiles. Ionized gas escapes the core region in an outflow to the north and south. Toward the south the outflow is partially limited by neutral material, producing a southern, spherical continuum component which exhibits much narrower H66α line profiles than the core region.

Subject headings: H II regions — ISM: individual (NGC 7538) — ISM: kinematics and dynamics — radio lines: ISM — stars: formation

1. INTRODUCTION

After the collapse of molecular cloud material, a newly formed star begins to interact with the surrounding molecular cloud. The details of the interaction between newly formed stars and molecular clouds are not well understood. Observational studies of the early stages of massive star formation may lead to a better understanding of this process.

Massive newly formed stars produce a large quantity of ultraviolet photons which photoionize nearby molecular cloud material. The photoionized H II regions are often observed in the radio continuum as ultracompact H II regions which typically have electron densities $\geq 10^4$ cm^{-3}, emission measures $\geq 10^7$ pc cm^{-6}, and diameters <0.1 pc (≈20,000 AU). When some star-forming complexes are observed with sufficient angular resolution and sensitivity, H II regions with sizes approximately an order of magnitude smaller are sometimes found (e.g., Gaume, Johnston, & Wilson 1993). We denote H II regions with diameters less than a few thousand AU as hypercompact.

NGC 7538 IRS 1 is an infrared source and hypercompact radio H II region in the NGC 7538 star formation complex at a distance of ≈3 kpc (Crampton, Georgelin, & Georgelin 1978). The core of NGC 7538 IRS 1 has been resolved into two radio lobes separated by 0.″2 (Turner & Matthews 1984; Campbell 1984). A weaker, spherical, 0.″5 diameter, continuum component is located a few 0.″1 to the south of the double core. The morphology of the NGC 7538 IRS 1 core prompted Campbell (1984) to propose that the double radio lobes are the two halves of a collimated outflow from a massive star. Many molecular line studies have been made of the region. NGC 7538 IRS 1 is associated with a large variety of molecular maser species, for example, OH (e.g., Dickel et al. 1982), H_2O (e.g., Kameya et al. 1990), CH_3OH (Menten et al. 1986), H_2CO (Rots et al. 1981), NH_3 (Madden et al. 1986), and $^{15}NH_3$ (e.g., Gaume et al. 1991). Interferometric imaging of quasi-thermal molecular emission has been made for ^{13}CO, HCO^+, HCN (see Pratap, Snyder, & Batrla 1992), and NH_3 (Henkel, Wilson, & Johnston 1984). These studies indicate a complex spatial and kinematic distribution of molecular material in the vicinity of NGC 7538 IRS 1 with an average local standard of rest (LSR) velocity in the range -57 to -67 km s^{-1}.

To understand the detailed interaction between NGC 7538 IRS 1 and the nearby molecular material, the velocity of the ionized gas must be determined. Toward this end Gaume et al. (1991) presented H76α, H42α, and H35α recombination line observations of the ionized gas toward NGC 7538 IRS 1 and IRS 2. The observations of each of these radio recombination lines indicate that the NGC 7538 IRS 1 H II region is redshifted between 20 to 40 km s^{-1} with respect to the surrounding molecular cloud. This surprising result prompted Gaume et al. (1991) to propose that the ionized gas of NGC 7538 IRS 1 is photoevaporating off the foreground molecular cloud and is channeled in a direction away from Earth. However, the signal-to-noise ratio of the Gaume et al. (1991) recombination line data is marginal. Therefore, we have obtained high-sensitivity, 0.″1 spatial resolution observations of the H66α recombination line toward NGC 7538 IRS 1 to further investigate the unusual recombination line emission and to better

[1] US Naval Observatory, 3450 Massachusetts Avenue, NW, Washington, DC 20392-5420.
[2] Code 7213, Naval Research Laboratory, Washington, DC 20375-5351.
[3] National Radio Astronomy Observatory, P.O. Box 0, Socorro, NM 87801.
[4] Astronomy Department, 1002 West Green Street, University of Illinois, Urbana, IL 61801.
[5] Max-Planck-Institut für Radioastronomie, Postfach 2024, D-53010 Bonn, Germany.

understand the relationship between NGC 7538 IRS 1 and the surrounding molecular cloud.

2. OBSERVATIONS AND DATA REDUCTION

The observations were made in two 10 hr sessions on 1992 December 12 and 20 using the Very Large Array (VLA)[6] telescope of the National Radio Astronomy Observatory (NRAO). At the time of the observations, the VLA was in the A configuration, which provides baseline lengths from 0.68 to 36.4 km. Our observations are not sensitive to source structures larger than $\sim 2''$.

The NGC 7538 IRS 1 region was observed for a total on-source time of approximately 14 hr at the rest frequency of the H66α line (22364.174 MHz). The central pointing position for these observations was R.A. = $23^h11^m36^s.65$, decl. = $+61°11'49''.9$ (1950.0). The source 3C 286 served as an absolute flux density calibrator; the flux density was assumed to be 2.56 Jy at the observing frequency. The source 2229+695 (0.38 Jy) was monitored frequently as a phase calibrator.

The recombination line observations were made in a VLA spectral line mode with a selected bandwidth of 25 MHz separated into 32 channels of width 781.25 kHz (10.5 km s^{-1}). The spectral resolution of the observations after Hanning weighting was 20.9 km s^{-1}. Channel 16 was set to an LSR velocity of -40 km s^{-1}. The data for the two observing sessions were inspected, edited, and calibrated independently of each other using the NRAO Astronomical Image Processing System (AIPS) software as implemented on NRL and NRAO computer systems. Bandpass calibration was accomplished using hourly observations of 3C 84 (28.0 Jy). After calibration, the data for the two observing sessions were combined for the self-calibration and imaging steps. The channel zero data, which contain the inner 75% of the original 25 MHz band, were Fourier inverted and then CLEANed in the standard manner. This channel contains both line and continuum emission. The maximum line contamination in the channel zero data is 8%; a more typical value is $\approx 5\%$. The channel zero data will henceforth be referred to as continuum data. To increase the dynamic range of the resulting images, two iterations of phase self-calibration were applied to the continuum data. The antenna-based gain corrections obtained from the continuum data were later applied to the spectral line database.

The self-calibrated continuum data were Fourier inverted using both "natural" and "uniform" weighting of the u, v data. Natural weighting of the u, v data results in greater overall sensitivity, and greater sensitivity to extended structure, with lower spatial resolution. The rms noise level and full width at half-maximum (FWHM) beam size of the continuum images resulting from natural and uniform weighting of the data are 0.2 mJy beam^{-1}, $0''.11$, and 0.4 mJy beam^{-1}, $0''.06$, respectively.

To obtain "line-only" images a linear fit to the continuum emission was performed in the visibility plane using three frequency channels at the redshifted end and two channels at the blueshifted end of the line-plus-continuum spectral database. The fit was then subtracted from visibilities in all the channels to produce a line-only data set (Cornwell, Uson, & Haddad 1992). These data were then Fourier inverted using natural weighting and CLEANed in the standard manner. The rms noise level and FWHM beam size for the spectral line images are 0.5 mJy beam^{-1} and $0''.11$, respectively.

It was found that the H66α recombination line emission toward NGC 7538 IRS 1 filled most of the 25 MHz bandwidth chosen for the 1992 December observations. To confirm this result and to assure a proper continuum subtraction, additional observations of the H66α line toward NGC 7538 IRS 1 were obtained 1993 February 27 in the VLA B configuration. The observing parameters were similar to those for the two observing sessions in 1992 December, except that a wider bandpass was employed and this session was 3 hours. The spectral line mode employed eight Hanning weighted channels across a 50 MHz bandpass, resulting in a velocity resolution of 83.8 km s^{-1}. These wider bandpass observations confirmed and validated our 25 MHz observations (§ 3.2).

3. DISCUSSION

3.1. *Continuum Emission*

Figures 1*a* (Plate 34) and 1*b* detail the continuum structure of NGC 7538 IRS 1. The north-south extent of the H II region is $\approx 1''.4$ (4000 AU). The hypercompact core has a size of $\approx 0''.4$ (1100 AU) and dominates the continuum emission. The core appears to be composed of two components in the lower resolution, naturally weighted image. These components are labeled in Figure 1*b* as the northern and southern core. A weaker, less compact component is located $0''.4$ to the south of the southern core. This feature is labeled the "south, spherical" region in Figure 1*b*. Continuum emission north of the core appears to extend nearly $0''.5$ to the northwest. Neither of the latter two extended components is well represented in the higher resolution, uniformly weighted image. The higher resolution (180 AU) image in Figures 1*a* and 1*b* resolves the double core into numerous bright emission clumps; these range in flux density from ≈ 10 to 19 mJy beam^{-1}. There are a few emission "holes" or "bays" in the core region. The brightness within these holes is ≈ 6 to 8 mJy beam^{-1}. From the naturally weighted data, beam-averaged peak continuum brightness temperatures are on the order of 10,000 K for the core. Beam-averaged peak continuum brightness temperatures are 12,000 K to 15,000 K for the brighter clumps in the core seen in the higher resolution uniformly weighted image. In § 3.3 we propose that the clumpy spatial distribution of the continuum emission may be attributed to photoionization of clumpy nearby molecular material. Based on our data, we cannot exclude the possibility that each of the continuum clumps seen in the uniformly weighted data represent the site of an individual ionizing star of O or B spectral type. However, we view this as an unlikely occurrence; see § III of Campbell (1984) for a more extensive discussion of this point.

It is instructive to compare our continuum data for NGC 7538 IRS 1 with the 2 cm data of Turner & Matthews (1984) and Campbell (1984). A direct comparison is warranted since our naturally weighted 1.3 cm image has nearly the same spatial resolution as these 2 cm data. First we note that there is disagreement on the absolute position of each of these three observations at the $0''.3$ level. However, the absolute position of NGC 7538 IRS 1 in our 1.3 cm images closely matches that of the $0''.2$ resolution 1.3 cm observations of Gaume et al. (1991). Although comparison of the general morphology of NGC 7538 IRS 1 seen in the two 2 cm observations and our 1.3 cm observation is quite favorable, a detailed comparison of the northern

[6] The VLA is a facility of the National Radio Astronomy Observatory, which is operated by Associated Universities, Inc., under cooperative agreement with the National Science Foundation.

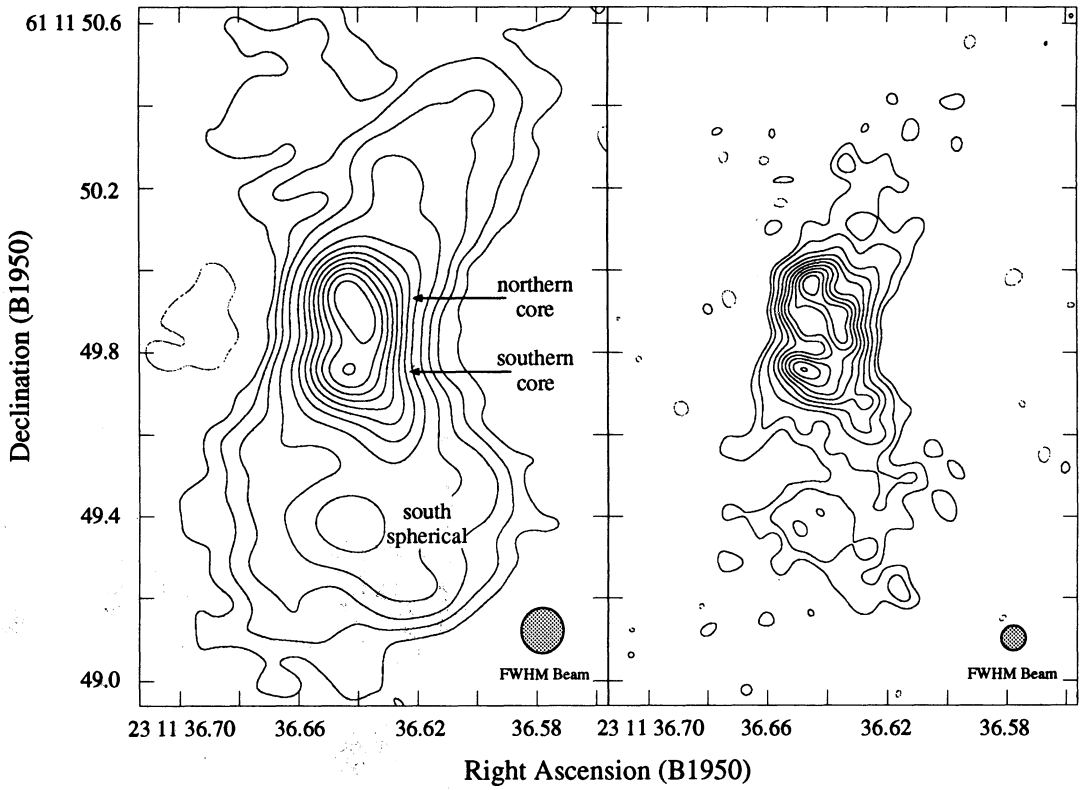

FIG. 1*b*

FIG. 1.—(*b*) Contour maps of the natually (*left*) and uniformly (*right*) weighted images shown in Fig. 1*a* (Plate 34). Natural weighting of the *u*, *v* data results in greater overall sensitivity and greater sensitivity to extended structure, with coarser spatial resolution. The peak and rms flux densities and FWHM size of the restoring beam for each image are 44 mJy beam $^{-1}$, 0.2 mJy beam^{-1}, 0.″11 (*left panel*) and 19 mJy beam^{-1}, 0.4 mJy beam^{-1}, 0.″06 (*right panel*). Contour levels for the left panel are -1, 1, 2.5, 5, 10, 20, ... 90% of the peak flux density. Contour levels for the right panel are -5, 5, 10, 20, ... 90% of the peak flux density. The northern and southern core and "southern, spherical" components are labeled in the left-hand panel.

and southern core regions does show some differences. Both of the 2 cm continuum images (Fig. 6 of Turner & Mathews 1984; Fig 3 of Campbell 1984) show the northern core as a simple pointlike region. Our 1.3 cm naturally weighted image shows the northern core to be elongated, with an axial ratio of 1.5:1. From our 0.″06 resolution uniformly weighted image, the northern core is composed of several clumps. Thus, we suggest that the difference in the 2 cm and 1.3 cm morphologies (but not the overall position shift) could be attributed to a greater 2 cm continuum optical depth for some individual clumps within the northern core.

The overall spectral index of NGC 7538 IRS 1 has been discussed by several authors (Pratap et al. 1992; Schilke et al. 1990). Pratap et al. (1992) have proposed a two-component model for NGC 7538 IRS 1. In their model the spectrum of one component, corresponding to our "south, spherical" region, has a turnover frequency near 3.7 cm. The other component, corresponding to our core regions, has a turnover frequency near 0.7 cm. Flux density comparisons between our 1.3 cm data and that of Turner & Matthews (1984) and Campbell (1984) are relevant. The peak and integrated flux densities of our 1.3 cm naturally weighted data (42 mJy beam^{-1}, 420 mJy) agree very well with those reported at 2 cm by Campbell (1984) but are a factor 1.3 higher than those reported at 2 cm by Turner & Matthews (1984). It appears that the mean turnover frequency for the core of NGC 7538 IRS 1 is at a wavelength of 1.3 cm or longer. Thus, the mean optical depth of the core of NGC 7538 IRS 1 is of order 1 near 1.3 cm. However, as noted in the previous paragraph there is evidence that a few individual clumps, particularly in the northern core, may have an optical depth somewhat greater than the mean.

3.2. *H66α Recombination Line Emission*

Recombination line emission was detected toward the core and "south, spherical" component of NGC 7538 IRS 1. Spectra of the H66α line emission toward the core region are shown in Figure 2*a* superposed on a contour plot of the continuum emission. The spectral line data base is comprised of images with 0.″02 × 0.″02 pixels. Each spectrum shown in Figure 2*a* is taken from an individual 0.″02 × 0.″02 pixel. However, for simplicity we have displayed spectra only for every other pixel. Thus, the spectra shown in Figure 2*a* are on a 0.″04 spatial grid. To increase the signal-to-noise ratio we have spatially integrated the H66α line emission over the two boxed areas in Figure 2*a*. These integrated spectra are shown in Figure 2*b*. The third spectrum in Figure 2*b* was integrated over a 0.″2 × 0.″2 region centered on the "south, spherical" component. The vertical bars in Figures 2*a* and 2*b* indicate the $\pm 1\ \sigma$ noise levels for the spectra. Figure 3*a* is a gray-scale representation of the velocity integrated H66α line-to-continuum ratio overlayed on contours of the continuum emission. The gray-scale image was obtained by dividing the zero moment image (integrated line intensity) by the continuum image. Figure 3*b* is a gray-scale representation of the H66α

PLATE 34

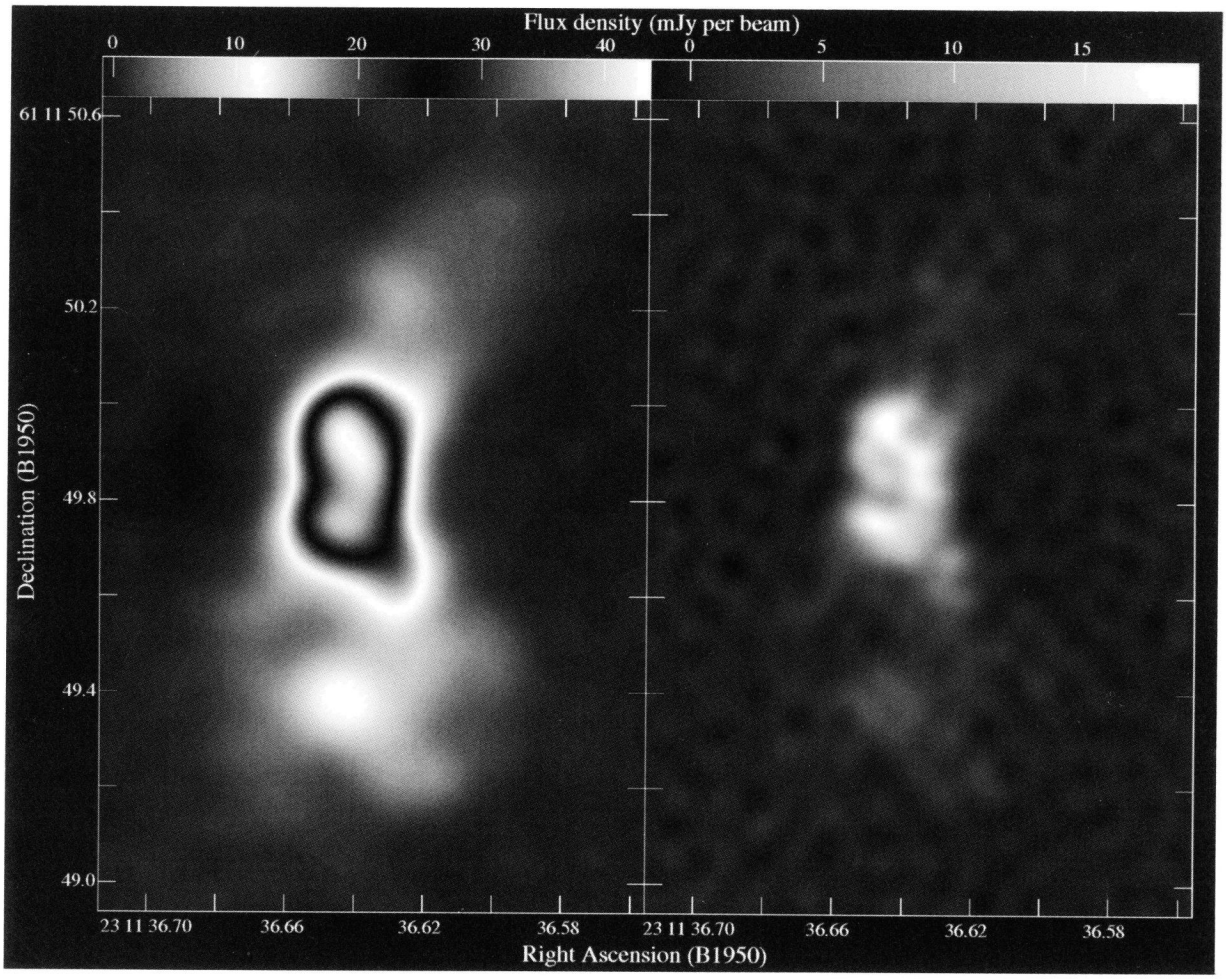

FIG. 1*a*

FIG. 1.—(*a*) Continuum images of NGC 7538 IRS 1 at a wavelength of 1.3 cm. The image shown in the left-hand panel was Fourier inverted using natural weighting of the *u*, *v* data. The image in the right-hand panel was inverted using uniform weighting of the *u*, *v* data. The transfer function of the naturally weighted image was "doubled" to emphasize weak features. The brightness temperatures reach 15,000 K for the clumpy core components seen in the right-hand image. Contour maps of these images are shown in Fig. 1*b* (see text).

GAUME et al. (see 438, 778)

recombination line second-moment image (velocity dispersion) overlayed on contours of the continuum emission. For a Gaussian-shaped line profile the second moment is the Gaussian FWHM divided by a factor of 2.4.

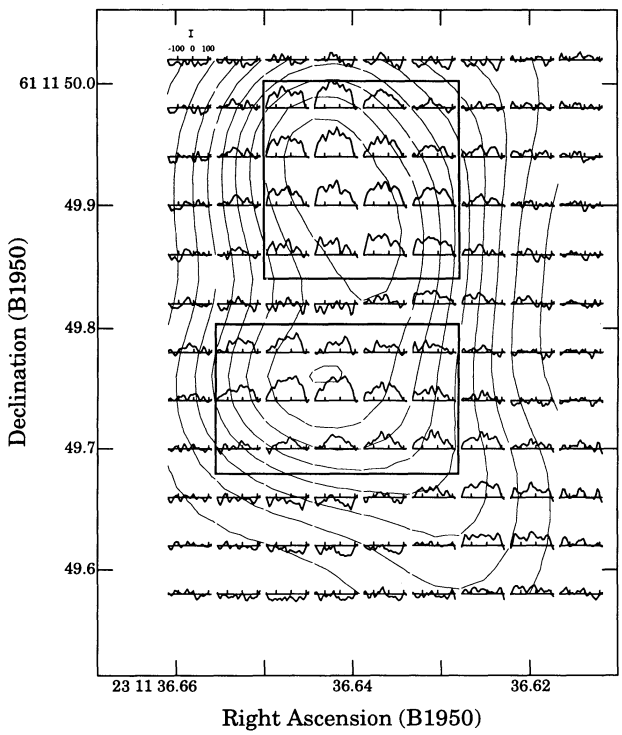

FIG. 2a

There are several striking aspects to the H66α line emission toward NGC 7538 IRS 1. Perhaps the most unusual aspect is the extreme width of the line profiles in the core region. The FWHM and full width at zero power (FWZP) line widths in the northern and southern regions of the core are ≈180 km s^{-1} and ≈250 km s^{-1}, respectively. The line from the core region fills a significant fraction of the 25 MHz bandpass. Our 50 MHz bandwidth observations (see § 2) confirm the wide line widths seen in the 25 MHz bandwidth data. The H66α line overlaps with the He66α line, shifted by 122 km s^{-1}. The helium line is expected to be significantly weaker than the hydrogen line, but the contribution of the helium line to the composite profile cannot be determined from our data. Pressure broadening of the H66α line is negligible, ≪2% of the total line width, given electron temperatures in the range of 10^4 K and electron densities in the range 10^4–10^5 cm^{-3}. The extreme line widths in the core region are caused by large motions of ionized material. The line width of the emission in the "south, spherical" region is considerably narrower, ≈50 km s^{-1}.

The spectral profiles for the northern and southern core regions are multiple peaked (Figs 2*a* and 2*b*), with many of the individual peaks significantly above the rms noise level. Multiple peaks may be seen in profiles for individual spectra (Fig. 2*a*) but are more easily seen in the integrated spectra (Fig. 2*b*) which have a better signal-to-noise ratio. Thus, the H66α line emission toward the northern and southern core regions cannot be adequately described by a single-component Gaussian model, since the profiles are very complex. We suggest a simple intepretation where the peaks of the recombination lines in the northern and southern core regions result from multiple, blended velocity components.

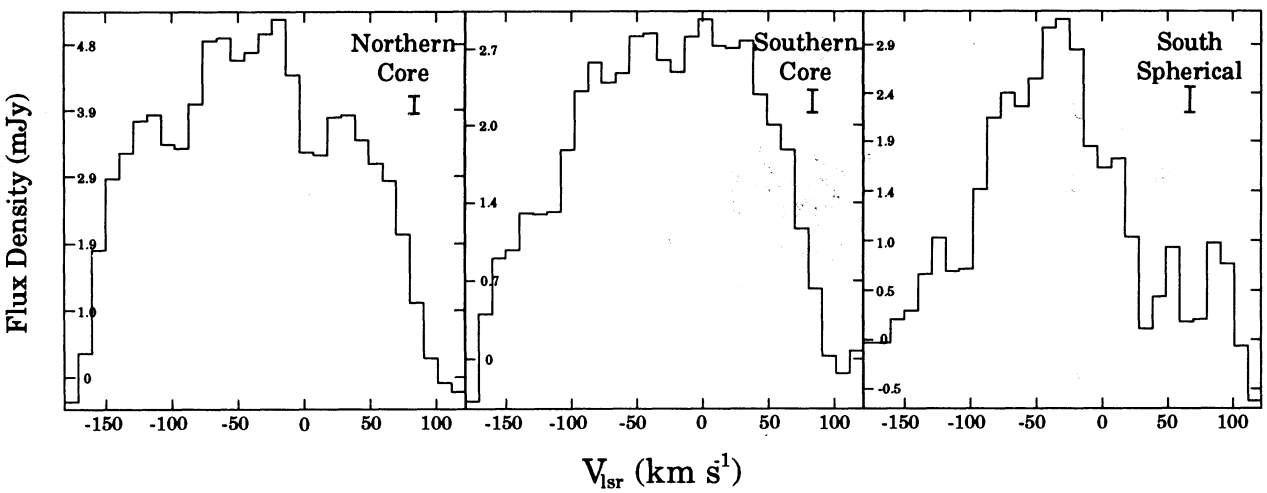

FIG. 2b

FIG. 2.—(*a*) Spectra of the H66α recombination line toward the continuum core of NGC 7538 IRS 1 overlayed on contours of the continuum emission. Note the unusual width of the lines, variations in the line-to-continuum ratio, and changes in the profile as a function of position within the core. The spectra are evenly distributed in a 0.″04 grid. The restoring beam applied to these data has a FWHM of 0.″11. The spatial location of each spectrum within the right ascension, declination grid is defined as the left-hand edge of the velocity axis. The range in flux density of the profiles is 4.5 to −2.1 mJy $beam^{-1}$. The profiles cover a velocity range of −176.1 to 117.1 km s^{-1}. Tick marks on the velocity axis are at ±100 and 0 km s^{-1}; these are labeled in the upper left-hand spectrum. The 1 σ noise for each spectrum is 0.5 mJy $beam^{-1}$. The vertical bar above the upper left spectrum indicates the ±1 σ noise level. The contours of the continuum emission are identical to those in Fig. 1*b*. The boxed areas indicate regions within the northern and southern core regions over which data were averaged to produce the spectra in (*b*). (*b*) Integrated spectra of the H66α recombination line toward NGC 7538 IRS 1. The boxed areas in (*a*) indicate the spatial regions over which data were averaged to produce the two leftmost spectra (indicated by northern and southern core). The rightmost spectrum (indicated by south, spherical) was produced by integrating over a 0.″2 × 0.″2 region centered on the "south, spherical" continuum peak, near R.A. = $23^h11^m36^s.64$, decl. = +61°11′49.″38. The 1 σ noise levels for the spectra are 0.12, 0.10, and 0.13 mJy from left to right, respectively. The vertical bars associated with each spectrum indicate the ±1 σ noise level. Note the striking difference in line width between the two spectra from the core region and the spectrum from the "south, spherical" continuum component.

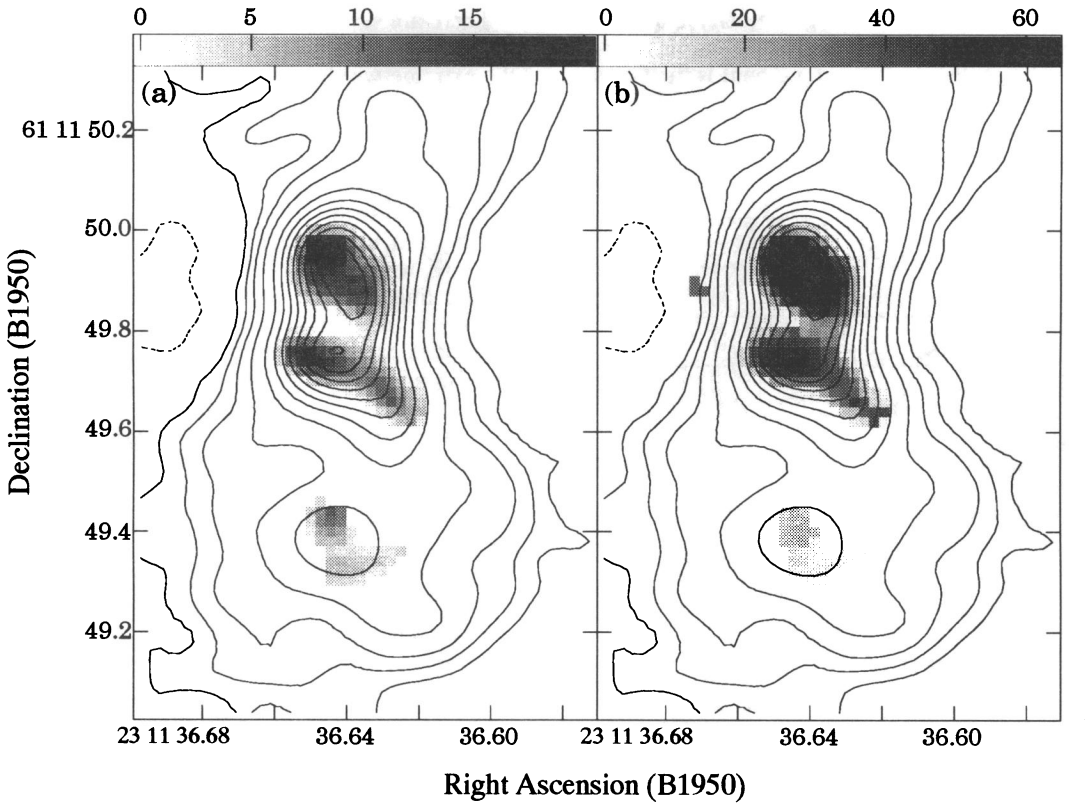

FIG. 3.—(*a*) Gray-scale representation of the velocity integrated line-to-continuum ratio overlayed on contours of the continuum emission obtained by dividing the zeroth moment image by the continuum image. The scale ranges from 0 to 20 km s^{-1}. The thin strip of smaller integrated line-to-continuum ratio midway between the northern and southern components of the core delineates a region of higher electron density. The continuum contours are the same as for Fig. 1*b*. (*b*) Gray-scale representation of the second moment image of the H66α line emission toward NGC 7538 IRS 1. The gray scale ranges from 0 to 64 km s^{-1}. For a Gaussian line profile the Gaussian FWHM is a factor of ≈2.4 larger than the second moment. Linewidths are considerably more narrow for the "south, spherical" continuum component than for the northern and southern core regions.

The change in the shape of the composite profile as a function of position is noteworthy. One can easily see that the relative intensities of the individual peaks within the composite spectrum change as a function of position (Figs. 2*a* and 2*b*). The peaks in the northern core integrated spectrum (Fig. 2*b*) are symmetric about the −50.5 km s^{-1} channel. The spectrum toward the southern core is asymmetric, with the largest intensities in redshifted velocities, near 33.3 km s^{-1} (see Fig. 2*a*). The change in the shape of the profiles as a function of position may be easily interpreted as changes in the relative intensities of the blended velocity peak components at various lines of sight through the core region.

One of the goals of these observations is to determine the velocity of the NGC 7538 IRS 1 ionized gas with respect to that of the surrounding molecular material. The determination of the characteristic velocity of the ionized gas is made more difficult by the extreme width and multiple-peak components in the spectral profiles (Fig. 2*a* and 2*b*) and coarse velocity resolution (20.9 km s^{-1}). Perhaps the best characterization of the velocity of the NGC 7538 IRS 1 ionized gas is that of the central, or average, velocity of the composite spectrum. An examination of individual and area-integrated spectra shows that the velocity centroid of the H66α emission remains remarkably constant with position within NGC 7538 IRS 1 (≈ −40 to −60 km s^{-1}).

Besides the unusually large line widths and profiles, the peak H66α line-to-continuum ratios are in the range of 8% to 10% for the core and 14% for the "south, spherical component." The electron temperatures calculated under the assumption of local thermodynamic equilibrium (LTE) are ≈3600 K, 4800 K, and 7500 K for the northern and southern core and "south, spherical" components. With an expected continuum opacity in the range of 1 to 2 for the core, the corrected LTE electron temperatures are reduced by a factor of 0.6 to 0.4. Since the continuum brightness temperature of the core in the naturally weighted image is ≈10,000 K, the emission measures (EM) of the peaks are $\approx 2 \times 10^9$ cm^{-6} pc. It is possible that line masering will be prominent if the electron density (n_e) is low. Following the methods outlined by Roelfsema & Goss (1992) and using the b_n and β_n values tabulated by Walmsley (1990), a non-LTE calculation was made to determine the range of electron temperatures and densities that are required to produce the observed H66α line emission. From a comparison of the results from model calculations with the observed profiles from the northern and southern cores (Fig. 2*b*), electron temperatures must be in the range of 10,000 K to 15,000 K and n_e must be in the range $10^{4.5}$ to 10^5 cm^{-3}.

As seen in Figure 3*a*, there is a thin region or strip of lower line-to-continuum ratio midway between the northern and southern core components. The peak line-to-continuum ratio in this strip is very small (<3%). Continuum levels at this location are as high as 80% of maximum. If the electron densities in this thin strip are an order of magnitude larger than for the northern and southern core, then the line flux density predicted by our non-LTE calculations is a factor of 4 to 5 times weaker, because the line intensities are closer to local ther-

modynamic equilibrium than is the case at lower densities. Thus, the thin strip of lower line-to-continuum ratio between the northern and southern core likely delineates a region of higher electron density. At this position the n_e must be in excess of 10^5 cm^{-3}.

3.3. *Models for NGC 7538 IRS 1*

Based on single-dish and interferometric observations of several radio recombination line transitions at centimeter and millimeter wavelengths, Gaume et al. (1991) find the line emission from NGC 7538 IRS 1 to be redshifted with respect to the velocity of the molecular cloud. The largest redshift of nearly 40 km s^{-1} is found for the H76α transition. Line widths were found to be <50 km s^{-1}. Gaume et al. (1991) explained the redshift by proposing that the ionized gas of NGC 7538 IRS 1 is photoevaporating off the foreground molecular cloud and is channeled in a direction away from Earth. In contrast to these previous data, the H66α recombination lines are extremely wide and multiple peaked. The centroid of the H66α spectrum is not consistent with the 40 km s^{-1} redshift determined for the H76α transition. Differences between the current recombination line data and that of Gaume et al. (1991) may be attributed to several factors. The single-dish H35α profile presented by Gaume et al. (1991) blends the emission from NGC 7538 IRS 1 with the much stronger emission from NGC 7538 IRS 2, found $\approx 8''$ to the north. The individual contributions from IRS 1 and IRS 2 are difficult to separate. The higher spatial resolution interferometric H42α and H76α recombination line data reported by Gaume et al. (1991) have much poorer sensitivity than the current H66α line data. Besides sensitivity, opacity effects are likely another cause of the difference between the H76α data of Gaume et al. (1991) and the current H66α line data. The combination of opacity effects and low signal-to-noise ratio may have biased the H76α data of Gaume et al. (1991) toward detection of one of the more redshifted emission features seen in our H66α profiles. Some differences between the H42α data and the current H66α data may be attributed to difficulty with subtraction of the continuum emission for the H42α line. Typical radio recombination lines seldom exceed 100 km s^{-1} FWZP. In the case of the H42α line, channels near the edges of the bands were assumed to contain line-free continuum emission. These channels in fact contain line emission due to the extraordinary width of the NGC 7538 IRS 1 recombination lines. Follow-up observations of the H39α recombination line are presented by Fritz et al. (1992). These H39α profiles are in better agreement with the current H66α data than the previously published H42α profiles. However, these data are also affected by inadequate continuum subtraction and low signal-to-noise ratio.

Campbell (1984) proposed that the double-lobed structure of NGC 7538 IRS 1 may be explained as a stellar wind outflow. In this model, a disk collimates and channels the stellar wind to the north and south. Evidence consistent with a disk structure is found in the infrared data of Hackwell, Grasdalen, & Gehrz (1982). A molecular structure elongated in the east-west direction has been imaged in ^{13}CO by Scoville et al. (1986), and a similar spatial distribution is seen in the HCN maps, of Pratap, Batrla, & Snyder (1989). This has been interpreted as a rotating torus. Based on 2 cm continuum data, Campbell (1984) suggested that the thickness of the disk is a few tens of AU, and the inner radius is ≈ 65 AU. Our higher spatial resolution, uniformly weighted, 1.3 cm image demonstrates that the continuum structure of the core is more complex than that of a simple double. It is difficult to identify the position of the proposed disk from our continuum data. However, evidence for a possible disk may be seen in the H66α line data. As discussed in § 3.2 the thin strip of lower line-to-continuum ratios found between the northern and southern core (Fig. 3*a*), delineates a region of significantly higher electron density. The position of this region is roughly that of the disk proposed by Campbell (1984).

Hollenbach et al. (1994) have proposed that many compact H II regions form by the photoevaporation of neutral accretion disks that orbit the newly born OB stars. This model may be relevant to our discussion because of the evidence for a possible disk associated with NGC 7538 IRS 1. In this model an accretion disk serves as a source of dense molecular material; the central star photoevaporates material off the surface of the disk. The hot, overpressured ionized material then flows away from the neutral disk. This model incorporates the case of both weak and strong stellar winds. For a freely flowing wind, the disk photoevaporation model results in a frequency spectrum with a spectral index α of 0.6 ($S \propto \nu^{\alpha}$). However, NGC 7538 IRS 1 does not exhibit a spectral index of 0.6 at centimeter wavelengths; the core of NGC 7538 IRS 1 is optically thick between 6 cm and 2 cm (Campbell 1984) and has an optical depth of order 1 between 2 cm and 1.3 cm (see § 3.1). Hollenbach et al. (1994) suggest that a steeper spectral index could still be consistent with the disk photoevaporation model if the ionized wind from the disk is trapped by ambient material. In any case, molecular line studies show that the spatial distribution of neutral material in the vicinity of NGC 7538 IRS 1 is significantly more complex than that of a thin disk. Thus, the idealized disk photoevaporation model cannot be directly applied to NGC 7538 IRS 1.

Our new continuum and recombination line data suggest that the Campbell (1984) and Gaume et al. (1991) models proposed for NGC 7538 IRS 1 require revision. We propose that a model capable of explaining the current observations must involve an ionized stellar wind outflow along with photoevaporation from a clumpy distribution of neutral material. As in the Campbell (1984) model, we suggest that the exciting star is located in the densest portion of the core component which has an unresolved, edge-on, disklike distribution. This dense distribution of material is seen as a thin strip of lower line-to-continuum ratio midway between the northern and southern core components (Fig. 3*a*; § 3.2). The extremely wide H66α recombination lines trace a stellar wind outflow from the central exciting star. Assuming modest opening angles for the outflow, the velocity of the wind must be on the order of a few 100 km s^{-1} to explain the extreme width of the H66α recombination lines. The ionized gas escapes the core region in an outflow to the north and south (see Figs. 1*a* and 1*b*). To the north the continuum emission extends at least 2″ (Fig. 1 of Campbell 1984). In the south the outflow is at least partially "capped" (i.e., blocked by neutral material) resulting in the "south, spherical" continuum component. The H66α lines are narrower at the position of the "south, spherical" component because there is little large-scale motion of the ionized gas. The 1.3 cm line in the "south, spherical" component is reasonably fitted by a single-component Gaussian with a central velocity of ≈ -55 km s^{-1} and a FWHM of ≈ 50 km s^{-1}. Although most of the masers are associated with the molecular material near the northern and southern core continuum components, some of the OH masers are found at the edges of the "south, spherical" component (Dickel et al. 1982), in the interface region between the outflow and the molecular "cap."

A freely expanding ionized wind is expected to have a rather smooth continuum appearance and exhibit a relatively smooth recombination line profile. Instead, the higher spatial resolution (0".06 = 180 AU) uniformly weighted continuum image (Fig. 1*a*) shows a clumpy continuum distribution and the H66α recombination line profiles are multiple peaked (Figs 2*a* and 2*b*). We have previously noted (§ 1) that NGC 7538 IRS 1 is surrounded by a complex distribution of dense molecular material. The existence of molecular masers in the material surrounding NGC 7538 IRS 1 implies densities in excess of 10^5 cm^{-3}. We propose that the molecular material surrounding NGC 7538 IRS 1 partially confines and channels the hot stellar wind. If the wind velocity is $\approx$300 km s^{-1}, we find the mass loss rate is $\approx 2 \times 10^{-4}\ M_\odot$ yr^{-1} by applying the formula of Smith et al. (1987). This mass-loss rate is extremely large, assuming all the ionized gas originates in a mass-loss wind arising from the central, exciting star. Alternatively, we suggest that photons from the central star photoionize the surrounding clumpy neutral molecular material. The gas which photoevaporates from this molecular material produces dense, localized pockets of hot ionized gas. These pockets of gas make a significant contribution to the observed continuum flux density and give the continuum emission (Fig. 1*a*) a clumpy appearance when imaged with high angular resolution (180 AU). The ionized gas photoevaporated from the surrounding molecular material interacts with, and becomes entrained in the stellar wind outflow. This results in a complicated, extremely broad, and multiple-peaked set of blended spectral profiles. Variations in the line profiles result from changes in the relative intensities of the emission from the various clumps/slabs at particular lines of sight through the core region. Thus, as discussed in § 3.2, the velocity centroid of individual spectra are the best determinant of the overall velocities of the ionized gas with respect to the molecular cloud. Determinations of the velocity centroids are difficult with the current data, but these appear to lie between -40 km s^{-1} and -60 km s^{-1} throughout the core region. This indicates that there are likely no significant velocity differences between the ionized gas and the molecular cloud.

In certain respects NGC 7538 IRS 1 appears to be quite similar to MWC 349, a radio source which has been suggested to be either an evolved object (White & Becker 1985) or the site of a recently formed star (Hamman & Simon 1986). MWC 349 exhibits an hourglass-shaped continuum morphology strongly suggesting the presence of a thin disk of neutral material. The spectral index of MWC 349 is 0.6. Martín-Pintado et al. (1993) have modeled the 1.3 cm continuum and H66α recombination line emission from MWC 349 as arising in a bipolar constant velocity expanding ionized wind. Non-LTE effects are a significant factor in the formation of the H66α line from MWC 349. In regard to the ionized gas, the main practical difference between MWC 349 and NGC 7538 IRS 1 appears to be the presence of a more complex distribution of dense molecular material surrounding NGC 7538 IRS 1. Whereas the ionized gas flows relatively unimpeded in MWC 349, resulting in a spectral index of 0.6, the ionized gas in NGC 7538 IRS 1 is confined and channeled by the nearby molecular material. Photoevaporated molecular material makes a significant contribution to the total amount of ionized gas present in NGC 7538 IRS 1. The presence of dense neutral material nearby the ionized gas lends weight to the argument that NGC 7538 IRS 1 is younger than MWC 349. The higher density in the NGC 7538 IRS 1 ionized gas prevents the larger deviations from LTE found in MWC 349.

4. CONCLUSIONS

We have imaged the 1.3 cm continuum and H66α line emission from NGC 7538 IRS 1 with a spatial resolution of 300 AU (0".1 at 3 kpc). The continuum emission toward the core region of NGC 7538 IRS 1 shows two bright core components. There is an extension of the continuum emission to the northwest of the core and a spherical component south of the core. When imaged with 180 AU resolution, the two core components are resolved into many emission clumps. The beam-averaged brightness temperature of the peak clumps is $\approx$15,000 K.

The H66α line data show extremely wide line profiles in the core region of NGC 7538 IRS 1, where the FWZP reaches 250 km s^{-1}. This line width indicates an expansion, or outflow, of ionized material. The profiles exhibit multiple emission peaks. The line shape changes significantly as a function of position within the core region. Non-LTE calculations show that non-LTE effects are significant in the formation of H66α lines from the core of NGC 7538 IRS 1. The change in line-to-continuum ratio within the core region is noteworthy. A region of significantly larger electron density is located midway between the northern and southern core regions; this is the position of the neutral disk proposed by Campbell (1984). The "south, spherical" continuum component exhibits much narrower line widths; this component can be fitted with a single-component Gaussian model with a velocity similar to that of the surrounding molecular material.

We propose that a model capable of explaining the current observations must involve a stellar wind outflow along with photoevaporation from a clumpy distribution of neutral material surrounding NGC 7538 IRS 1. The exciting star is located in the densest portion of the core component which has an unresolved, edge-on disklike distribution. The extremely wide H66α recombination lines trace a stellar wind outflow from the central exciting star. The velocity of the outflow is on the order of a few 100 km s^{-1}. The ionized gas escapes the core region in an outflow to the north and south. In the south the outflow is at least partially limited, resulting in much narrower line widths in the "south, spherical" continuum component.

The mass-loss rate is $\approx 2 \times 10^{-4}\ M_\odot$ yr^{-1}, assuming all the ionized gas originates in a mass-loss wind directly from the central, exciting star. We suggest that much of the ionized gas results from photoevaporation of the surrounding clumpy molecular material by photons from the central, exciting star. The clumps seen in the high-resolution continuum image are explained as pockets of ionized gas recently photoevaporated from clumpy neutral material. The ionized gas photoevaporated from the surrounding molecular material interacts with, and becomes entrained in, the ionized stellar wind outflow. This results in a complicated, extremely broad, and multiple-peaked set of blended spectral profiles. Variations in the line profiles result from changes in the relative intensities of the emission from the various clumps/slabs at particular lines of sight through the core region. The velocity centroid of the recombination line emission appears to be the best parameter for characterizing the overall velocity of the ionized gas with respect to the molecular cloud. Contrary to previous, more limited observations of the recombination line emission toward NGC 7538 IRS 1, there is no significant velocity difference between the ionized gas and the molecular cloud.

The authors thank D. Mehringer for assistance in calculating the non-LTE models and P. Benaglia for assistance at an early stage of the data reduction process. R. A. G. wishes to thank P. F. Bowers for many useful discussions on star formation in general and NGC 7538 IRS 1 in particular. Basic research in Radio Interferometry at the Naval Research Laboratory is supported by the Office of Naval Research. H. R. D. acknowledges partial support from grant NSF AST 90-21034 and from the Laboratory for Astronomical Imaging at the University of Illinois under grant AST 90-24603. T. L. W. and K. J. J. were supported in part by the Max-Planck-Forschungspreis, administered by the A. von Humboldt-Stiftung.

REFERENCES

Campbell, B. 1984, ApJ, 282, L27
Crampton, D., Georgelin, Y. M., & Georgelin, Y. P. 1978, A&A, 66, 1
Cornwell, T. J., Uson, J. M., & Haddad, N. 1992, A&A, 258, 583
Dickel, H. R., Rots, A. H., Goss, W. M., & Forster, J. R. 1982, MNRAS, 198, 265
Fritz, M., Dickel, H. R., Wright, M. C. H., & Goss, W. M. 1992, BAAS, 24, 797
Gaume, R. A., Johnston, K. J., Nguyen, H. A., Wilson, T. L., Dickel, H. R., Goss, W. M., & Wright, M. C. H. 1991, ApJ, 376, 608
Gaume, R. A., Johnston, K. J., & Wilson, T. L. 1993, ApJ, 417, 645
Hackwell, J. A., Grasdalen, G. L., & Gehrz, R. D. 1982, ApJ, 252, 250
Hamman, F., & Simon, M. 1986, ApJ, 311, 909
Henkel, C., Wilson, T. L., & Johnston, K. J. 1984, ApJ, 282, L93
Hollenbach, D., Johnstone, D., Lizano, S., & Shu, F. 1994, ApJ, 428, 654
Kameya, O., Morita, K., Kawabe, R., & Ishiguro, M. 1990, ApJ, 355, 562
Madden, S. C., Irvine, W. M., Matthews, H. E., Brown, R. D., & Godfrey, P. D. 1986, ApJ, 300, L79
Martín-Pintado, J., Gaume, R. A., Bachiller, R., Johnston, K. J., & Planesas, P. 1993, ApJ, 418, L79
Menten, K. M., Walmsley, C. M., Henkel, C., Wilson, T. L., Snyder, L. E., Hollis, J. M., & Lovas, F. J. 1986, A&A, 169, 271
Pratap, P., Batrla, W., & Snyder, L. E. 1989, ApJ, 341, 832
Pratap, P., Snyder, L. E., & Batrla, W. 1992, ApJ, 387, 241
Roelfsema, P. R., & Goss, W. M. 1992, A&A Rev., 4, 161
Rots, A. H., Dickel, H. R., Forster, J. R., & Goss, W. M. 1981, ApJ, 245, L15
Schilke, P., Mauersberger, R., Walmsley, C. M., & Wilson, T. L. 1990, A&A, 227, 220
Scoville, N. Z., Sargent, A. I., Sanders, D. B., Claussen, M. J., Masson, C. R., Lo, K. Y., & Phillips, T. G. 1986, ApJ, 303, 416
Smith, H., Fischer, J., Geballe, T. R., & Schwartz, P. R. 1987, ApJ, 316, 265
Turner, B. E., & Matthews, H. E. 1984, ApJ, 277, 164
Walmsley, C. M. 1990, A&AS, 82, 201
White, R. L., & Becker, R. H. 1985, ApJ, 297, 677